

# Histopathological and biochemical assessment of liver damage in albino Wistar rats treated with cytotoxic platinum compounds in combination with 5-fluorouracil

Nusrat Bano<sup>1</sup>, Rahila Najam<sup>2</sup>

<sup>1</sup>Department of Pharmacology, King Saud Bin Abdulaziz University For Health Sciences, Jeddah, Saudi Arabia

<sup>2</sup>Department of Pharmacology, University of Karachi, Karachi, Saudi Arabia

**Submitted:** 25 December 2016

**Accepted:** 20 April 2017

Arch Med Sci 2019; 15 (4): 1092–1103

DOI: <https://doi.org/10.5114/aoms.2019.86064>

Copyright © 2019 Termedia & Banach

## Corresponding author:

Nusrat Bano PhD  
Department of Pharmacology  
King Saud Bin  
Abdulaziz University  
For Health Sciences  
King Abdulaziz  
Medical City  
National Guard Health  
9515 Jeddah, Saudi Arabia  
Phone: +96 6560240886  
E-mail: [banonu@ngha.med.sa](mailto:banonu@ngha.med.sa)

## Abstract

**Introduction:** Chemotherapy-induced hepatotoxicity in cancer patients often results in cessation of therapy and prevents completion of the treatment plan. The entire pathological description and comparison of hepatic damage induced by oxaliplatin or cisplatin in combination with 5-fluorouracil (5-FU) is not adequately reported. This study reports histopathological assessment of hepatotoxicity of a non-tumor bearing organ in rats treated with 5-FU, oxaliplatin and cisplatin (CDDP).

**Material and methods:** Changes in hepatic biochemical profile of 36 albino Wistar rats equally divided into different treatment groups with cisplatin, oxaliplatin, 5-FU, cisplatin plus 5-FU and oxaliplatin plus 5-FU were compared with a group of rats treated with normal saline (control group). At the end of treatments, hepatic tissues were taken for blinded histopathological assessment by light microscopy.

**Results:** Serum glutamate pyruvate transaminase and serum glutamic-oxaloacetic transaminase levels were disrupted in rats treated with 5-FU alone and in combination with cisplatin or oxaliplatin. Hepatocellular injuries, e.g. sinusoidal dilatation, venular fibrosis and centrilobular vein injury induced by oxaliplatin were intensified in treatment groups also receiving 5-FU, manifested as massive architectural distortion, periportal fibrosis, hepatic cord degeneration and cystic lesions with demarcated margins. Hepatocellular degenerative sequence and abnormally dilated central hepatic vein was shown in the cisplatin plus 5-FU treatment group with hemorrhage and blood filled sinusoids.

**Conclusions:** Oxaliplatin-associated cystic lesions were intensified in rats treated with a combination of 5-FU and oxaliplatin.

**Key words:** cisplatin, chemotherapy, hepatic, oxaliplatin, toxicity.

## Introduction

Oxaliplatin and 5-fluorouracil (5-FU) are key components of first line chemotherapy in colorectal carcinoma (CRC), which is the second and third leading cause of cancer in women and men respectively [1]. 5-FU as a single cytotoxic agent has limited therapeutic activity [2] but in combination with oxaliplatin it is the most effective and frequently used agent in metastatic CRC [3]. 5-FU in combination of cisplatin (CDDP) is

an effective chemotherapeutic regimen indicated for larynx preservation (induction chemotherapy) [4] and head and neck cancer [5].

Platinum compounds are considered to be the most effective agents in cancer chemotherapy [6]. Cisplatin and oxaliplatin are first and third generation platinum analogues respectively, which act by inhibiting DNA synthesis. 5-FU, on the other hand, is a pyrimidine analogue, which irreversibly inhibits thymidylate synthase [7]. 5-FU is metabolically inactivated by dihydropyrimidine dehydrogenase (DPD) in the hepatic cells [8]. Adverse hepatic manifestations induced by oxaliplatin and 5-FU interfere largely with factors of efficacy and tolerability in CRC treatment. Histological changes and vascular hepatic lesions in non-tumor bearing liver cells are associated with oxaliplatin based neoadjuvant chemotherapy in combination with 5-FU [9]. Rubbia-Brandt *et al.* [10] reported sinusoidal dilatation and obstruction, sinusoidal barrier rupture and veno-occlusive fibrosis in resected metastatic liver of colorectal cancer patients treated with oxaliplatin. Therapeutically adequate doses of oxaliplatin in CRC with liver metastases have adverse implications for non-tumor bearing liver cells since intrinsic chemosensitivity of oxaliplatin is attenuated in hepatocellular cancer cells as compared to normal cells due to impaired gap junction function mediated by connexin proteins (Cx26) [11].

Chemotherapy-induced hepatotoxicity has varying outcomes. Liver laboratory test findings are usually abnormal in cancer patients undergoing chemotherapy [12]. 5-FU based cancer chemotherapy is even reported to reactivate hepatitis B virus [13]. Chemotherapy-induced hepatic injury is caused by reactive oxygen species (ROS) production, required for cytotoxic action on tumor cells [14]. ROS-mediated lipid peroxidation with protein carbonyl formation leading to oxidative stress in mitochondria (isolated from rat liver) incubated with oxaliplatin is also reported [15].

Histopathological assessment of hepatocellular damage induced by oxaliplatin in combination with 5-FU is not adequately reported in the literature. Furthermore, the degree of hepatic damage induced by the combination of 5-FU and oxaliplatin is not compared with the combination of cisplatin and 5-FU. Rats, frequently used for animal model design in toxicological studies [16–18], can provide a clear spectrum of histologically assessed hepatocellular alterations with 5-FU treatment. This experimental study was designed to comparatively assess host of oxaliplatin, cisplatin and 5-FU induced liver cell damage alone and in combinations. The study also aimed to identify the individual effects of 5-FU, oxaliplatin and cisplatin on hepatocellular integrity in a toxicological rodent model.

## Material and methods

Thirty-six healthy, virgin and genetically isogenic male albino Wistar rats (*Rattus norvegicus*) weighing 180–260 g were selected from stock of inbred species (20 generations of brother × sister mating).

Experiments were conducted in Dow University of Health Sciences, Karachi following institutional and ethical approval. Ethical approval was granted by the Board of advanced studies and research, University of Karachi, Pakistan (Resol. no 226-A/Sc). Animal housing, bedding, handling and feeding were carried out in optimal environments of standardized animal house. Rats were kept in a spacious and well-ventilated facility (at reduced noise) with 10 : 14 light and dark cycle. Diffused lighting without flickering was provided. Temperature was maintained at  $\pm 23^{\circ}\text{C}$  without swings. Relative humidity was kept between 65 and 75% to avoid infections. Standard opaque polypropylene cages (wire mesh tops) were placed on appropriately positioned vibration proof cage racks, ensuring proper air exchange. Adequate adsorbent bedding (wood shaving) with appropriate depth and layering ( $0.5 \pm 2$  cm) free of parasitic, microbial and chemical contaminants was provided. Rats were accustomed to 'gentling' in a seven-day rest period. Nutritionally adequate and contamination-free feed (40% protein content) was provided. Food and tap water were provided *ad libitum*. Natural posture of feeding was allowed by foster foraging behavior. Additional food provided in the hopper was also sprinkled onto the cage floor bedding.

### Animal dosing protocol

Animals were divided into six treatment groups. A seven-day rest period with sufficient rat chow was assigned to each group. All rats were treated with intraperitoneal (IP) injection, which is preferred for oxaliplatin, cisplatin and 5-FU administration in rats [19–22]. IP is favored over the intravenous (IV) route (rat tail vein) because the maximal volume allowed by IV in rats is 5 ml/kg, whereas the maximal volume by IP can be up to 10 ml/kg [23]. Risk of extravasation is also high in the IV route for inflammatory and locally irritant chemotherapeutic agents.

Group A ( $n = 6$ ) was treated with normal saline solution (0.9% NS). It was the control group. Group B ( $n = 6$ ) was treated with 5-FU (15 mg/kg), whereas group C ( $n = 6$ ) received CDDP (0.8 mg/kg) [22]. Group D ( $n = 6$ ) was treated with oxaliplatin (0.8 mg/kg) [19, 24]. Group E ( $n = 6$ ) was treated with a combination of CDDP (0.8 mg/kg) + 5-FU (15 mg/kg). Group F ( $n = 6$ ) was treated with a combination of oxaliplatin (0.8 mg/kg) + 5-FU (15 mg/kg).

All groups were treated on days 1, 5, 10, 15 and 20. The drugs were given twice weekly for 2.5 weeks with a 2- and 3-day rest period after week 1 and week 2 respectively. The dosing range of the drugs was selected from similar toxicological studies in rats [19, 20, 25]. Injection was made at the lower right quadrant of the abdomen, close to the pelvic bone and midline of the xiphoid process, exercising caution to avoid the cecum, bladder or liver. The needle was inserted at a 30° angle as the shaft of needle reached a depth of 0.5 cm.

### Biochemical testing

Blood was sampled after 10 days of the last dose by cardiac puncture. The animal was deeply anesthetized using chloroform and checked for successful anesthesia by pinching the rat paw toe. Blood samples were collected in anticoagulant tubes (3 ml in green top heparinized tube; 3 ml in lavender top EDTA tube and 3 ml in light blue top citrate tube). Blood cells were separated from plasma by centrifugation for 10 min (1000–2000×g) in a refrigerated centrifuge machine. The centrifuge time was maintained at 10 min to avoid depletion of the platelets and attain designated plasma for serological testing immediately after transferring plasma into polypropylene tubes at a temperature of 2–8°C with Pasteur pipettes. Standardized biochemical testing kits were used to assess levels of TBR, DBR, ALKPO<sub>4</sub>, serum glutamate pyruvate transaminase (SGPT), serum glutamic-oxaloacetic transaminase (SGOT) and  $\gamma$ -glutamyl transferase (GGT).

### Sacrifice and organ excision

The rat was deeply anesthetized in a chloroform jar and laid out (ventral side up) on a dissection board. Feet were pinned by strong dissection pins, angled to place strain. Skin was laid back by pinching a skin fold in the mid ventral line to make an incision with a fine scalpel. The cut was continued forward to the level of the lower lip and backwards around the genitals. The lower scissor blade was kept within the skin and kept horizontal to prevent body wall damage. Pulling away the freshly dissected rat skin from the body wall, surgical cuts were made at a point forward along limbs, with pinned skin. As the exposed structures of pectoral muscles curved up from the chest to the arm and the outline of ribs, liver and intestines, the abdominal cavity was entered by pinching the wall and making a cut through down to the genitals and up to the xiphoid cartilage. The abdominal wall was dissected along line of the thorax defined by the lower ribs. From the top at the xiphoid cartilage, three lobes of the liver were visible. It was carefully removed and placed in ice cold buffered solution, dried and weighed immediately and preserved in

10% phosphate buffered formalin solution as an entire specimen in a single jar.

### Gross pathological assessment

Gross pathological assessment was made on color, size and surface marks. The cut surface was assessed for any apparent lesion/abnormal mass and representative sections were submitted in two cassettes for each sample. Representative section from livers (A-F) were cut and submitted in cassette 1 (A-F) and cassette 2 (A-F).

Slide preparation: Liver tissues (2–3 mm), fixed in 10% formaldehyde for slide preparation in saline phosphate buffer for 24 h, were placed in 70% isopropyl alcohol for 180 min and then in ascending strength of solution for 2 h each (80%, 90%, 100% isopropyl alcohol). The amount of alcohol was 15 times the size of the tissue. Tissues were dipped in acetone for 60–90 min and shaken periodically. After removing from acetone, xylene was added to check for milkiness. Dehydrated tissue was impregnated in molten paraffin wax at a temperature of 58–60°C. Molten paraffin was poured into L-Block along the tissues and hardened. Tissues were sectioned (2–8  $\mu$ m) using a microtome. Egg white and glycerin in equal amounts were beaten and filtered by adding 1% sodium salicylate to prepare Mayer's albumin solution. Tissues were mounted on the slides with Mayer's albumin solution and kept warm at 60° for 2 h. The slides were placed on a slide holder with paraffin sections. Slides were deparaffinized with xylene for 20–30 min, blotting out the excess. Tissues were rehydrated with descending grades of isopropyl alcohol 2–3 min each and placed in water for 3 min. Excess water was blotted and tissues were placed into hematoxylin stain for 1–2 min and then placed in tap water for 1–2 min. Slides with tissue sections were dipped in HCl and then Scott's water (sodium carbonate 3.5 g, magnesium sulfate 20 g and distilled water 1 l) for 1 min each and then in eosin stain for 30 s. Tissues were dehydrated in ascending grades of isopropyl alcohol followed by 20–30 min in xylene. Coverslips were placed using a drop of DPX mountant and dried overnight. Morphological assessment was inclusive of all cases on hematoxylin and eosin (H&E). Blinded histopathological assessment was made under bright field microscope with the components, Model U-MDOB3, SN6M02703, Olympus corporation (device complied with par 15 of FCC rules) and model LB×4 ITF, T5 SN 7A25800, Olympus corporation by a pathologist and the lead author.

### Statistical analysis

A paired sample test was used to analyze the data using the statistical software SPSS version

19.0. In the paired sample *t*-test, calculation of sample mean and standard deviation was followed by calculation of the test statistic and probability of observing the test statistic. Statistical significance is claimed at the cut-off value less than 0.05 to ensure 95% confidence in results. Values were considered as:  $p < 0.001$  (very highly significant),  $p < 0.01$  (very significant) and  $p < 0.05$  (significant).

## Results

### Biochemical assessment

Table I shows liver enzyme levels in each treatment group compared to the control group. SGOT and SGPT levels are sufficiently disrupted in 5-FU treated rats. The comparative difference from the control group is highly significant due to marked

**Table I.** Comparative changes in hepatic biomarkers in rat model of toxicity (paired samples test)

Acute toxicity			Paired differences		<i>T</i>	<i>df</i>	<i>P</i> -value
			Mean	Standard deviation			
L.F.T	Bilirubin total	Group A – Group B	-0.050	0.138	-0.889	5	0.415
		Group A – Group C	-0.217	0.147	-3.606	5	0.015
		Group A – Group D	-0.817	0.331	-6.041	5	0.002
		Group A – Group E	-0.917	0.160	-14.015	5	< 0.001
		Group A – Group F	-0.783	0.366	-5.248	5	0.003
	Bilirubin direct	Group A – Group B	-0.183	0.098	-4.568	5	0.006
		Group A – Group C	-0.033	0.103	-0.791	5	0.465
		Group A – Group D	-0.367	0.175	-5.129	5	0.004
		Group A – Group E	-0.450	0.164	-6.708	5	0.001
		Group A – Group F	-0.333	0.121	-6.742	5	0.001
	ALKP04	Group A – Group B	-8.333	16.330	-1.250	5	0.267
		Group A – Group C	25.333	8.189	7.577	5	0.001
		Group A – Group D	-88.000	10.789	-19.979	5	< 0.001
		Group A – Group E	-86.500	13.217	-16.030	5	< 0.001
		Group A – Group F	-198.000	18.308	-26.490	5	< 0.001
SGPT	Group A – Group B	-14.667	3.386	-10.609	5	< 0.001	
	Group A – Group C	-20.333	5.086	-9.793	5	< 0.001	
	Group A – Group D	-56.500	10.483	-13.202	5	< 0.001	
	Group A – Group E	-39.000	6.261	-15.258	5	< 0.001	
	Group A – Group F	-47.000	6.812	-16.901	5	< 0.001	
SGOT	Group A – Group B	-11.000	3.162	-8.521	5	< 0.001	
	Group A – Group C	-17.167	5.076	-8.284	5	< 0.001	
	Group A – Group D	-20.500	5.648	-8.891	5	< 0.001	
	Group A – Group E	-17.667	9.266	-4.670	5	0.005	
	Group A – Group F	-28.333	4.274	-16.238	5	< 0.001	
GGT	Group A – Group B	-0.333	3.559	-0.229	5	0.828	
	Group A – Group C	-11.667	6.088	-4.694	5	0.005	
	Group A – Group D	-16.833	6.853	-6.017	5	0.002	
	Group A – Group E	-9.500	7.232	-3.218	5	0.024	
	Group A – Group F	-21.167	6.274	-8.263	5	< 0.001	

*P*-value < 0.05 (significant), *p*-value < 0.01 (highly significant), *p*-value < 0.001 (very highly significant).

elevations in serum levels of ALKPO<sub>4</sub>, SGOT and SGPT in rats treated with 5-FU in combination with cisplatin and oxaliplatin. TBR and GGT levels were significantly raised in each treatment group except group B.

### Gross pathological assessment

Figure 1 A represents liver specimen A (NS treated rat) submitted in a single container in formalin measuring 4 × 3.5 cm with predominantly unremarkable surface. Figure 1 B shows liver specimen B (5-FU treated rat) submitted in a single container in formalin measuring 4 × 4 cm with remarkable surface. Sectioning exhibited grey white circumscribed area measuring 0.5 × 0.5 cm. Figure 1 C shows liver specimen C (cisplatin treated rat) submitted in a single container in formalin, measuring 4 × 3 cm and remarkable surface. Sectioning exhibited ulcerated grey white circumscribed area measuring 0.5 × 0.8 cm. Figure 1 D represents liver specimen D (oxaliplatin treated rat) was submitted in a single container in formalin. Single liver tissue measured 4.5 × 4 cm with remarkable surface. Cut surface exhibited two ulcerated grey white circumscribed areas measuring 0.5 × 0.5 cm each. Figure 1 E shows liver specimen E (cisplatin plus 5-FU treated rat) measured 4.5 × 4 cm with remarkable surface. Sectioning exhibited ulcerated grey white circumscribed area measuring 0.5 × 0.6 cm. Figure 1 F shows liver specimen F (oxaliplatin plus 5-FU treated rat) measured 5 × 3.5 cm with remarkable surface. Sectioning exhibited ulcerated grey white circumscribed area measuring 0.6 × 0.6 cm.

Three lobes of the liver (with intact blood supply) on top of xyphoid cartilage following laparotomy had visible appearance of peliotic hepatitis in rats treated with oxaliplatin with and without 5-FU (group D and F).

The lesions had an apparently darker tone (bluish black marbled) amidst brown colored hepatic tissues. Gross inspection of removed liver (oxaliplatin treated rat) revealed “Swiss cheese” appearance of phlebotatic peliotic lesions on cut sections. Similar compound peliotic lesions (phlebotatic or sinusoidal) in rats treated with combination of 5-FU and oxaliplatin (treatment group F) appeared as blood-filled spherical cavities thinly lined with fibrosis.

### Histopathological assessment of hepatotoxicity in albino Wistar rats

Figure 2 shows effects of 0.9% NS and 5-FU on rat liver. Effects of cisplatin is shown in Figure 3. Figure 4 shows effects of oxaliplatin, 5-FU + cisplatin and 5-FU + oxaliplatin on rat liver.

### 0.9% NS treated rats

Figure 2 A shows normal liver cells with central vein and opening of sinusoids in the central vein. Trabecular polygonal hepatocytes with abundant cytoplasm, Kupffer cells, sinusoids and endothelial cells, with no structural alterations are visible in Figures 2 B–D. Normal spherical nuclei with prominent nucleolus are represented in Figures 2 A–D. Some bi-nucleated hepatocytes are also visible in these cells. The basic lobular architecture is intact with no presentation of overt ataxia.

### 5-FU treated rats

Fibrocystic lesions with inflammatory cells and plasma are shown in group B. Figure 2 E shows the circumscribed lesion with fibrous vascular papillary core and central nuclei. Figure 2 F shows the circumscribed lesion in transition with the normal liver cells. Figure 2 G shows the same lesion at higher resolution. Figure 2 H shows chronic inflammatory cells, mostly plasma. Periportal inflammatory cells are visible without structural loss. Slight degree of hemorrhage between the sinusoids is observed. No defined nuclear changes without fragmentation are seen. Figure 2 I shows signs of chronic inflammation, scattered eosinophils and plasma cells which lie at the cyst boundary.

### Cisplatin treated rats

Figure 3 A shows dilated sinuses filled with erythrocytes. Figure 3 B shows focal dilated and congested blood vessels. Figures 3 C–E show perivenular proliferation of fibroblasts. Intact liver architecture in transition of fibrosis is visible in Figure 3 D. Figure 3 F shows a cystic lesion in transition with liver at 10× resolution. The cystic lesion is visible in Figure 3 G. Figure 3 H shows focal area of nuclear enlargement and pyknosis at fine resolution. All these changes are focal but overall the nucleus is intact. Appearance of very large nucleus with prominent nucleolus reveals the hepatic damage.

### Oxaliplatin treated rats

Figure 4 A shows the cystic lesion with the wall of inflammatory cells. Figure 4 B shows sinusoidal filling with RBC. Focal variability in nucleus size is also visible. Periportal inflammation can also be observed. Bi-nucleation of hepatocytes is observed. Figures 4 C and D show a clear picture of periportal perivascular inflammation. Figure 4 E shows the complete cystic lesion with predominant inflammatory margins.

### 5-FU + cisplatin treated rats

Figure 4 F shows abnormally enlarged nucleus with prominent nucleoli and features of pyknosis.

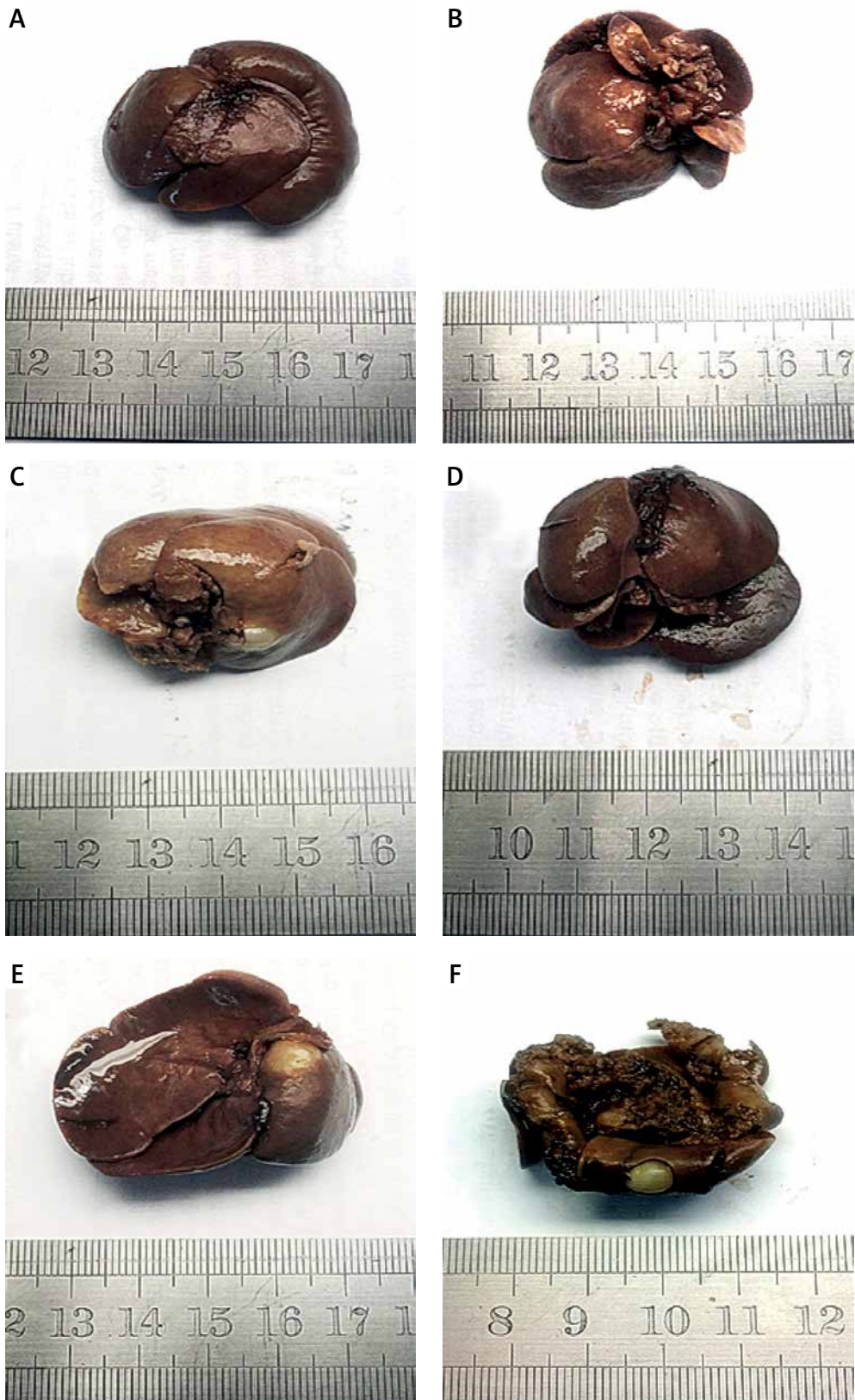


**Figure 1.** Gross pathological assessment of rat liver treated with 0.9% NS (A), 5-FU (B), CDDP (C), oxaliplatin (D), 5-FU + CDDP (E) and 5-FU + oxaliplatin (F)

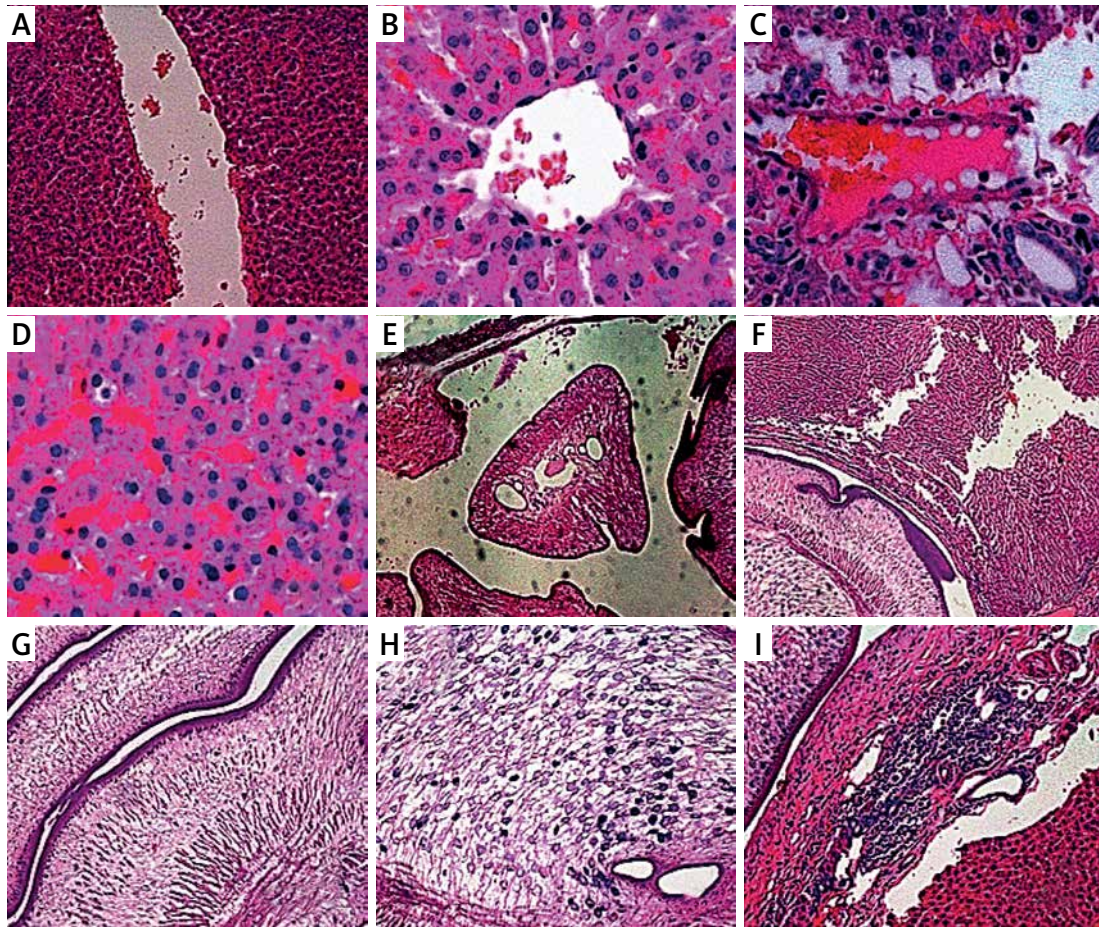


**Figure 2.** Histopathological effects of 0.9% normal saline (A–D) and 5-FU (E–I) on rat liver

Figure 4 G shows the variation in size and shape of the nucleus. Cytoplasmic vacuoles and degenerative sequence is seen. Blood filled sinusoids are visible. Figure 4 H shows abnormally dilated hepatic central vein.

#### 5-FU + oxaliplatin treated rats

Figures 5 A and B show abnormalities in the size and shape of the nucleus. Hepatocyte degeneration is clear and neutrophil infiltration is predominant. Figure 5 C shows vacuolization in the cytoplasm and focal nucleomegaly with prominent nucleoli. Figure 5 D shows enlarged nucleus associated with cytoplasmic vacuoles. Figure 5 E show neutrophilic infiltration, architectural distortion and cytoplasmic vacuoles. Figure 5 F shows cystic lesion with inflammatory margins at fine resolution.

#### Discussion

The present study investigated the biochemical and histopathological features of hepatic toxicity induced by 5-FU, cisplatin and oxaliplatin in rats. Gross liver inspection of oxaliplatin treated rats (group D) exposed peliotic hepatitis. Microscopic

findings further revealed irregular focal dilations of sinusoids. The cavernous lumen of the lesion was densely packed with blood. Tissues lining the dilated sinusoids were well preserved without necrotic cells. Similar findings in an oxaliplatin-treated cancer patient were reported by Uchino *et al.*, described as lesions characterized by injured centrilobular zones, mass defects and extremely severe sinusoidal dilatation in non-tumor bearing hepatic cells [26]. Morphological features of oxaliplatin-induced sinusoidal lesions had similarities to hepatic lesions in veno-occlusive disease with high dose chemotherapy [27]. Regenerative sequelae were apparently retarded in the oxaliplatin-treated group (group D), indicative of impaired hepatocyte proliferation, previously observed in oxaliplatin-treated Wistar rats following partial hepatectomy [28].

Distortion of the hepatic cord with compression of surrounding tissues was associated with a few hepatocellular nodules in oxaliplatin plus 5-FU (group F) treated rats. Light microscopy (group F) showed sinusoidal dilatation and hemorrhage along with coagulative necrosis. In 5-FU and oxaliplatin treated CRC patients, such sinusoidal obstructive syndrome (SOS), presenting as metachro-

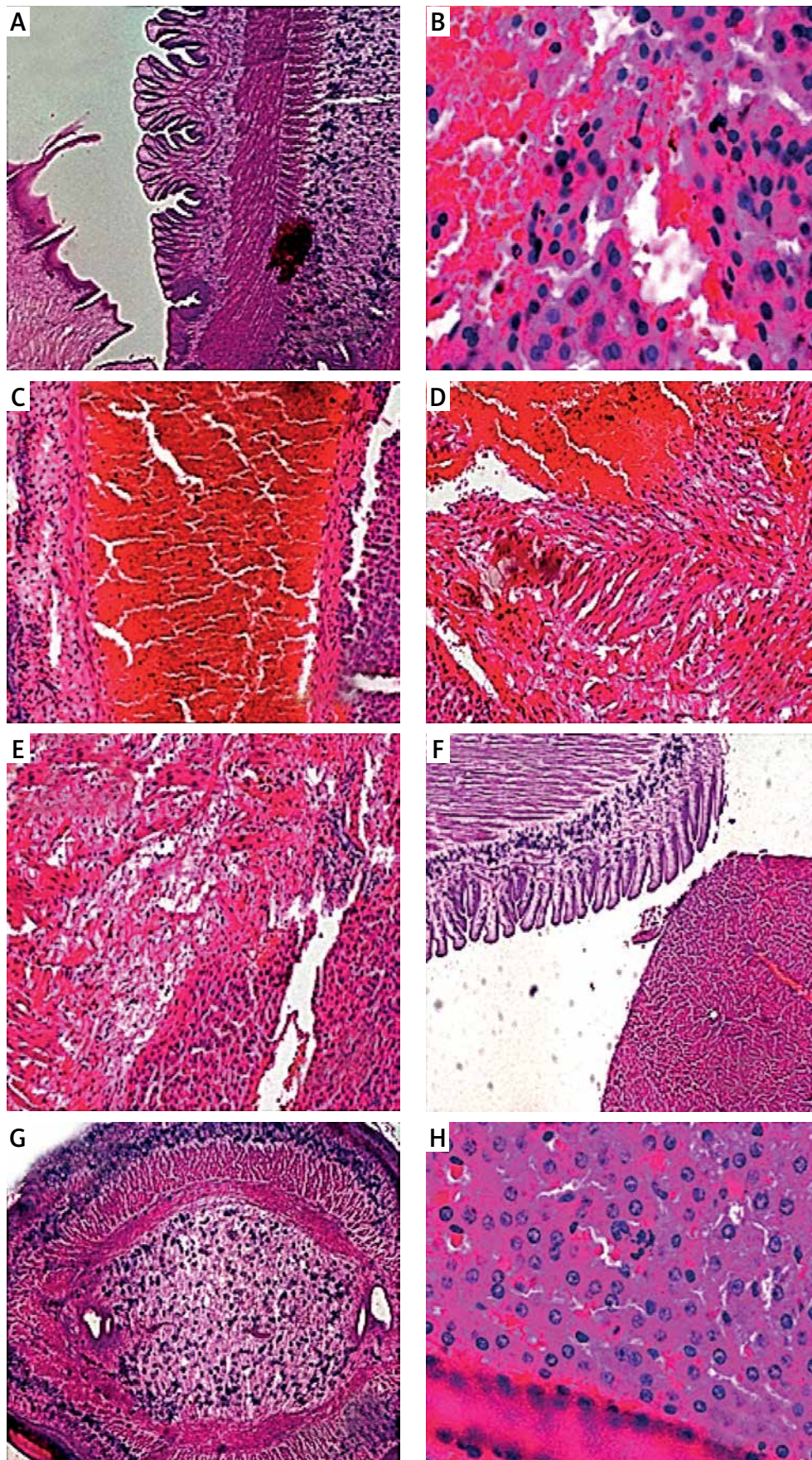


Figure 3. Histopathological effects of cisplatin on rat liver



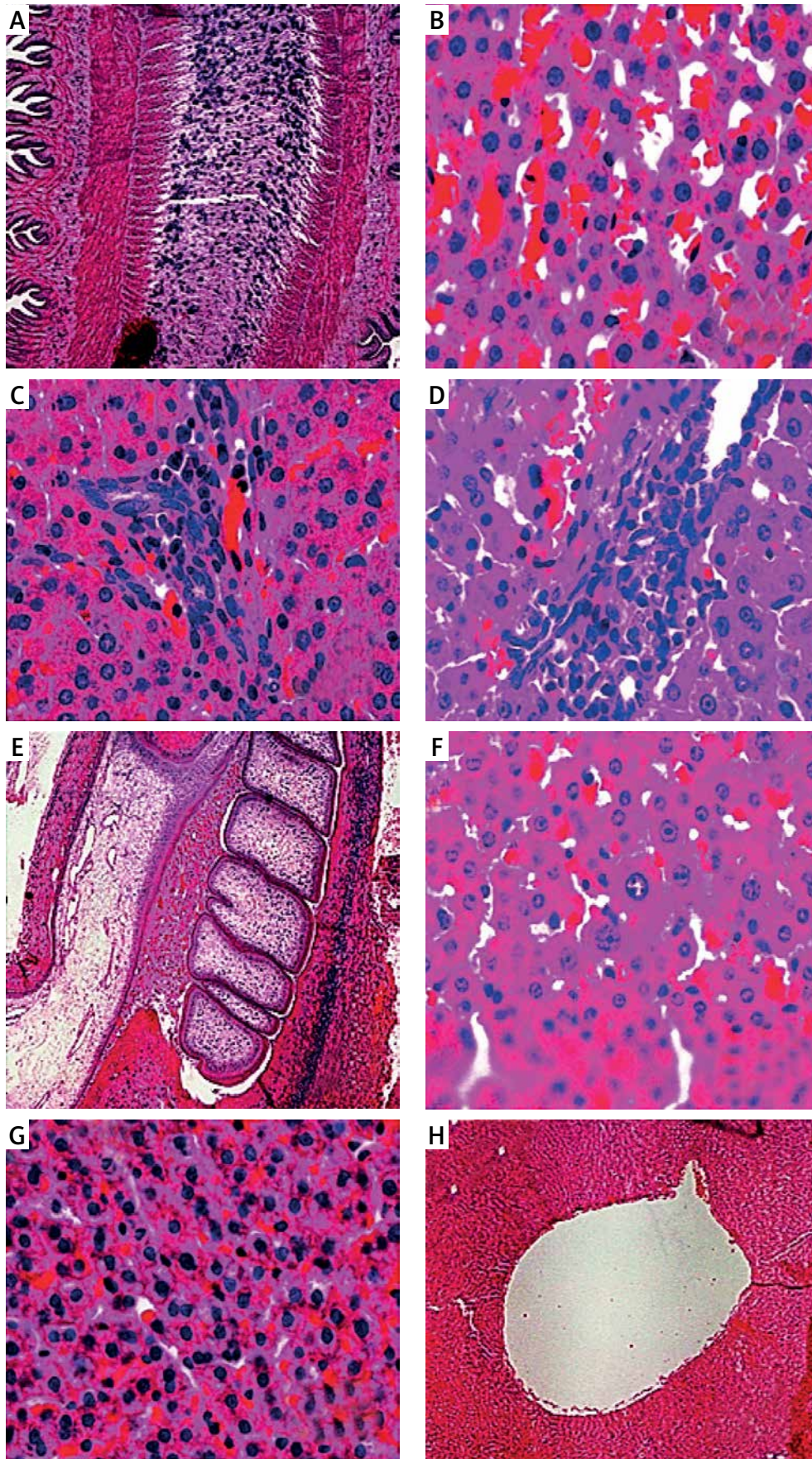
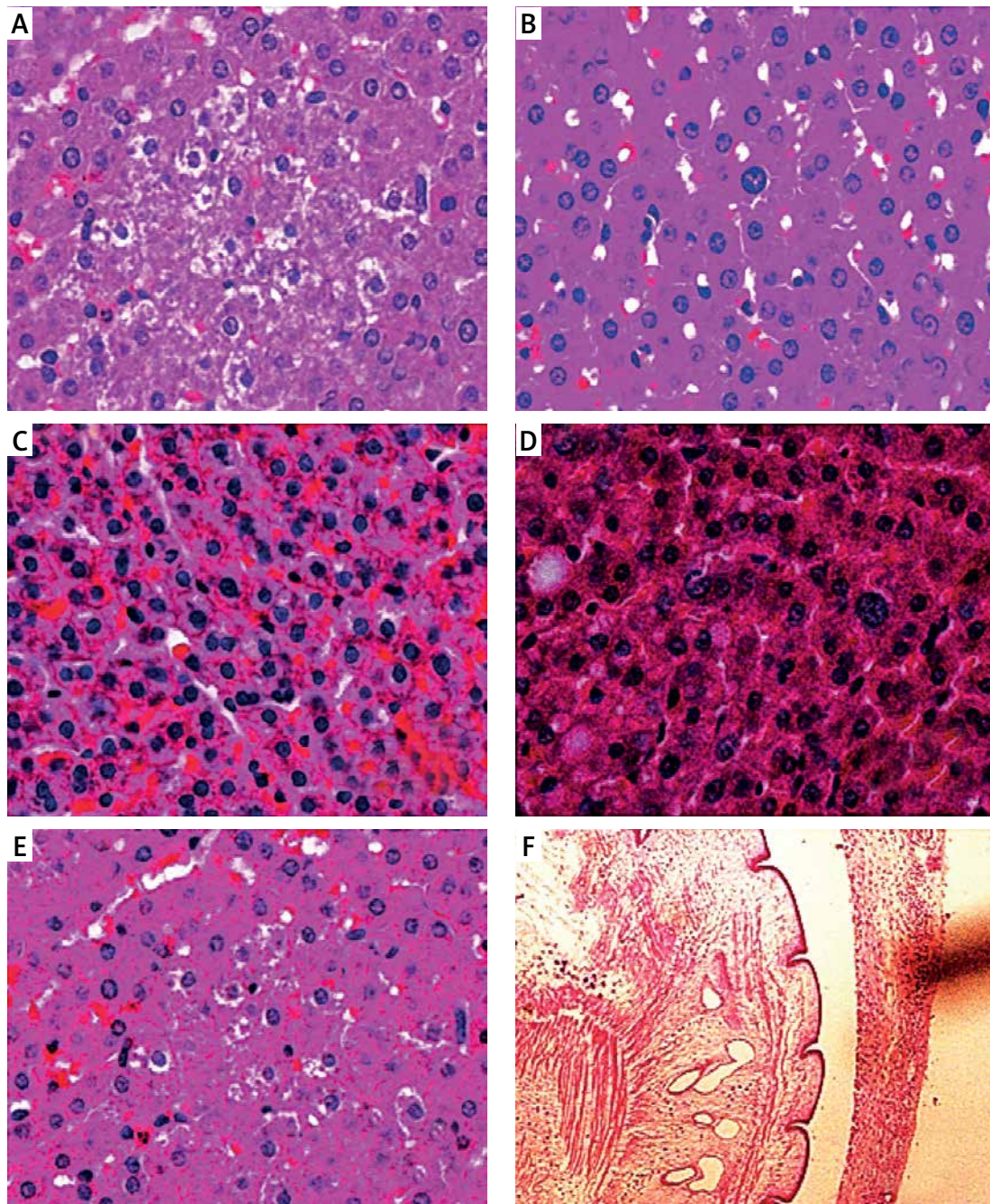


Figure 4. Histopathological effects of oxaliplatin (A-E) and 5-FU + cisplatin (F-H) on rat liver



**Figure 5.** Histopathological effects of 5-FU + oxaliplatin on rat liver

nous pseudotumor with unclear hypodense mass, mimics CRC metastasis and can be mistaken for it [29]. Pathogenesis of SOS induced by 5-FU and oxaliplatin in rodents is described by activation of the coagulation cascade, direct release of increased number of platelets into the circulation associated with elevated vWF expression and upregulated expression of factor X transcript in the animal liver [30]. Oxaliplatin-induced SOS is also related to activation of matrix metalloproteinase-9 (MMP9) [31]. This oxaliplatin-induced damage was apparently intensified when combined with 5-FU (group F) due to suppression or inhibition of the liver cell

regeneration and repair process induced by 5-FU [32]. On the other hand, rapid elimination of 5-FU (terminal half-life 8–20 min after IP administration) is reliant on swift catabolism of the drug in the liver [33]; therefore, changes in liver function due to toxicity of oxaliplatin may intensify 5-FU toxicity. Owing to the intertwined description of mechanisms involved in adverse drug reactions, it seems that both drugs contribute to adverse implications for liver profile when administered in combination.

5-FU induced direct hepatic toxicity in rats (group B), e.g. inflammation and necrosis with col-

lagenous fibril formation. Reduction in CYP2C6/11 expression at the levels of mRNA in 5-FU treated rats was recently reported by Fukuno *et al.* [34]. In a previous study, 5-FU treatment was also shown to decrease liver attenuation and cause fatty infiltration and steatosis [35]. Histological findings in this experiment provided substantial evidence that oxaliplatin-induced hepatic toxicity worsened when 5-FU was added to the cytotoxic regimen.

Cisplatin treatment induced considerable hepatotoxicity in rats (group C) with formation of prominent cystic lesions, perivenular proliferation of fibroblasts and focally dilated and congested blood vessels. Pyknosis and an abnormally enlarged nucleus were also noted with light microscopy. In the cisplatin plus 5-FU treatment group (group D), a similar pattern of damage was seen with marked intensity. Cystic lesion with predominant inflammatory margins, sinusoidal filling with hemorrhage, periportal perivascular inflammation and abnormalities in size and number of nucleoli were noted. These findings are in line with a previous study by Huang *et al.* [36], which reported cisplatin-induced hepatotoxicity in mice, manifested as excessive bleeding, hepatocyte vacuolation, necrosis, cytoplasmic degeneration, hepatocyte vacuolation, inflammatory cellular infiltration associated with elevated cytokine levels of iNOS, IL-6, TNF- $\alpha$  in liver and increased expression of caspase genes 3 and 9 (apoptotic related). Omar *et al.* [37] reported a decrease in p-Akt expression and increase in NF- $\kappa$ B expression in cisplatin-treated rats. Cisplatin-induced hepatocellular toxicity was caused by oxidative stress with increase in reactive oxygen species [38]. Alterations in the antioxidant defense system following cisplatin treatment are reported to associate with low levels of superoxide dismutase and reduced glutathione in the liver [39].

Cisplatin-induced liver toxicity was somewhat similar to liver cirrhosis as indicated by high levels of GGT and SGPT in cisplatin-treated groups (group C and E). Although 5-FU is recognized as a hepatotoxic agent, it was not previously reported to induce pseudocirrhosis [40]. In our study however, 5-FU was shown to aggravate cisplatin-induced hepatotoxicity. 5-FU is reported to exacerbate hepatocellular damage in liver cirrhosis related to elevation aminotransferases in occult fibrosis [41]. Thus, chemotherapy-induced hepatocellular toxicity in 5-FU based platinum regimens cannot be neglected in calculations of the risk-to-benefit ratio in cancer patients.

In conclusion, oxaliplatin-induced sinusoidal injuries are intensified in rats co-treated with 5-FU with a notable retardation in the degenerative sequence. Cisplatin plus 5-FU induced hepatic damage is more severe compared to individual drug treatment with cisplatin and 5-FU. 5-FU is thus shown to intensify liver toxicity in rats treated

either with first or third generation platinum analogs.

### Conflict of interest

The authors declare no conflict of interest.

### References

- Hubbard JM. Management of colorectal cancer in older adults. *Clin Geriatr Med* 2016; 32: 97-111.
- Yalcin S, Bayram F, Erdamar S, et al. Gastroenteropancreatic neuroendocrine tumors: recommendations of Turkish multidisciplinary neuroendocrine tumor study group on diagnosis, treatment and follow-up. *Arch Med Sci* 2017; 13: 271-82.
- Nagata N, Mishima H, Kurosawa S, et al. mFOLFOX6 plus panitumumab versus 5-FU/LV plus panitumumab after six cycles of frontline mFOLFOX6 plus panitumumab: a randomized phase ii study of patients with unresectable or advanced/recurrent, RAS wild-type colorectal carcinoma (SAPPHIRE) – study design and rationale. *Clin Colorectal Cancer* 2017; 16: 154-7.e1.
- Janoray G, Pointreau Y, Garaud P, et al. long-term results of a multicenter randomized phase iii trial of induction chemotherapy with cisplatin, 5-fluorouracil,  $\pm$  docetaxel for larynx preservation. *J Natl Cancer Inst* 2016; 108: djv368.
- Wang HM, Lin CY, Hsieh CH, et al. Induction chemotherapy with dose-modified docetaxel, cisplatin, and 5-fluorouracil in Asian patients with borderline resectable or unresectable head and neck cancer. *J Formos Med Assoc* 2017; 116: 185-92.
- Kutwin M, Sawosz E, Jaworski S, et al. Investigation of platinum nanoparticle properties against U87 glioblastoma multiforme. *Arch Med Sci* 2017; 13: 1322-34.
- Yu H, Liu Y, Pan W, Shen S, et al. Polyunsaturated fatty acids augment tumoricidal action of 5-fluorouracil on gastric cancer cells by their action on vascular endothelial growth factor, tumor necrosis factor-alpha and lipid metabolism related factors. *Arch Med Sci* 2015; 11: 282-91.
- Lunenburg CA, Henricks LM, Guchelaar HJ, et al. Prospective DPYD genotyping to reduce the risk of fluoropyrimidine-induced severe toxicity: ready for prime time. *Eur J Cancer* 2016; 54: 40-8.
- Aloia T, Sebah M, Plasse M, et al. Liver histology and surgical outcomes after preoperative chemotherapy with fluorouracil plus oxaliplatin in colorectal cancer liver metastases. *J Clin Oncol* 2006; 24: 4983-90.
- Rubbia-Brandt L, Audard V, Sartoretti P, et al. Severe hepatic sinusoidal obstruction associated with oxaliplatin-based chemotherapy in patients with metastatic colorectal cancer. *Ann Oncol* 2004; 15: 460-6.
- Yang Y, Zhu J, Zhang N, et al. Impaired gap junctions in human hepatocellular carcinoma limit intrinsic oxaliplatin chemosensitivity: a key role of connexin 26. *Int J Oncol* 2016; 48: 703-13.
- Ulcickas YM, Bortolini M, Casso D, et al. Incidence of liver injury among cancer patients receiving chemotherapy in an integrated health system. *Pharmacoepidemiol Drug Saf* 2015; 24: 427-34.
- Lin JW, Chang ML, Hsu CW, et al. Acute exacerbation of hepatitis C in hepatocellular carcinoma patients receiving chemotherapy. *J Med Virol* 2016; 89: 153-60.
- Bhakuni GS, Bedi O, Bariwal J, et al. Animal models of hepatotoxicity. *Inflamm Res* 2016; 65: 13-24.

15. Tabassum H, Waseem M, Parvez S, et al. Oxaliplatin-induced oxidative stress provokes toxicity in isolated rat liver mitochondria. *Arch Med Res* 2015; 46: 597-603.
16. Turkyilmaz S, Cekic AB, Usta A, et al. Ethyl pyruvate treatment ameliorates pancreatic damage: evidence from a rat model of acute necrotizing pancreatitis. *Arch Med Sci* 2019; 15: 232-9.
17. Çetin A, Çiftçi O, Otlu A. Protective effect of hesperidin on oxidative and histological liver damage following carbon tetrachloride administration in Wistar rats. *Arch Med Sci* 2016; 12: 486-93.
18. Kim MS, Lee S, Jung N, et al. The vitamin D analogue paricalcitol attenuates hepatic ischemia/reperfusion injury through down-regulation of Toll-like receptor 4 signaling in rats. *Arch Med Sci* 2017; 13: 459-69.
19. Mannelli LD, Zanardelli M, Failli P, et al. Oxaliplatin-induced neuropathy: oxidative stress as pathological mechanism. Protective effect of silibinin. *J Pain* 2012; 13: 276-84.
20. Al Moundhri MS, Al-Salam S, Al Mahrouqee A, et al. The effect of curcumin on oxaliplatin and cisplatin neurotoxicity in rats: some behavioral, biochemical, and histopathological studies. *J Med Toxicol* 2013; 9: 25-33.
21. Ling B, Coudoré-Civiale MA, Balayssac D, et al. Behavioral and immunohistological assessment of painful neuropathy induced by a single oxaliplatin injection in the rat. *Toxicology* 2007; 234: 176-84.
22. El-Sayyad HI, Ismail MF, Shalaby FM, et al. Histopathological effects of cisplatin, doxorubicin and 5-fluorouracil (5-FU) on the liver of male albino rats. *Int J Biol Sci* 2009; 5: 466-73.
23. Workman P, Aboagye EO, Balkwill F, et al. Guidelines for the welfare and use of animals in cancer research. *Br J Cancer* 2010; 102: 1555-77.
24. Joseph EK, Chen X, Bogen O, et al. Oxaliplatin acts on IB4-positive nociceptors to induce an oxidative stress-dependent acute painful peripheral neuropathy. *J Pain* 2008; 9: 463-72.
25. Cavaletti G, Petruccioli MG, Marmiroli P, et al. Circulating nerve growth factor level changes during oxaliplatin treatment-induced neurotoxicity in the rat. *Anticancer Res* 2001; 22: 4199-204.
26. Uchino K, Fujisawa M, Watanabe T, et al. Oxaliplatin-induced liver injury mimicking metastatic tumor on images: a case report. *Jpn J Clin Oncol* 2013; 43: 1034-8.
27. Rubbia-Brandt L, Lauwers GY, Wang H, et al. Sinusoidal obstruction syndrome and nodular regenerative hyperplasia are frequent oxaliplatin-associated liver lesions and partially prevented by bevacizumab in patients with hepatic colorectal metastasis. *Histopathology* 2010; 56: 430-9.
28. Hubert C, Dahrenmoller C, Marique L, et al. Hepatic regeneration in a rat model is impaired by chemotherapy agents used in metastatic colorectal cancer. *Eur J Surg Oncol* 2015; 41: 1471-8.
29. Kawai T, Yamazaki S, Iwama A, et al. Focal sinusoidal obstruction syndrome caused by oxaliplatin-induced chemotherapy: a case report. *Hepatitis* 2016; 16: e37572.
30. Robinson SM, Mann J, Vasilaki A, et al. Pathogenesis of FOLFOX induced sinusoidal obstruction syndrome in a murine chemotherapy model. *J Hepatol* 2013; 59: 318-26.
31. Okuno M, Hatano E, Nakamura K, et al. Regorafenib suppresses sinusoidal obstruction syndrome in rats. *J Surg Res* 2015; 193: 693-703.
32. Nagasue N, Kobayashi M, Iwaki A, et al. Effect of 5-fluorouracil on liver regeneration and metabolism after partial hepatectomy in the rat. *Cancer* 1978; 41: 435-43.
33. Diasio RB, Harris BE. Clinical pharmacology of 5-fluorouracil. *Clin Pharmacokinet* 1989; 16: 215-37.
34. Fukuno S, Nagai K, Kasahara K, et al. Altered tolbutamide pharmacokinetics by a decrease in hepatic expression of CYP2C6/11 in rats pretreated with 5-fluorouracil. *Xenobiotica* 2018; 48: 53-9.
35. Peppercorn PD, Reznik RH, Wilson P, et al. Demonstration of hepatic steatosis by computerized tomography in patients receiving 5-fluorouracil-based therapy for advanced colorectal cancer. *Br J Cancer* 1998; 77: 2008-11.
36. Huang TH, Chiu YH, Chan YL et al. Antrodia cinnamomea alleviates cisplatin-induced hepatotoxicity and enhances chemo-sensitivity of line-1 lung carcinoma xenografted in BALB/cByJ mice. *Oncotarget* 2015; 6: 25741-54.
37. Omar HA, Mohamed WR, Arafa ES, et al. Hesperidin alleviates cisplatin-induced hepatotoxicity in rats without inhibiting its antitumor activity. *Pharmacol Rep* 2016; 68: 349-56.
38. Cagin YF, Erdogan MA, Sahin N, et al. Protective effects of apocynin on cisplatin-induced hepatotoxicity in rats. *Arch Med Res* 2015; 46: 517-26.
39. Ateyya H, Yosef H, Nader MA. Ameliorative effect of trimetazidine on cisplatin-induced hepatotoxicity in rats. *Can J Physiol Pharmacol* 2016; 94: 225-30.
40. Lopes GL, Zucchetti BM, de Mendonça Rego JF, et al. Pseudocirrhosis after the use of taxanes and bevacizumab in metastatic breast cancer: case reports. *J Pharm Pharmacol* 2017; 5: 158-63.
41. Momiyama K, Nagai H, Ogino Y, et al. Glutathione for hepatotoxicity in patients with liver cirrhosis and advanced hepatocellular carcinoma receiving hepatic arterial infusion chemotherapy. *Clin Cancer Drugs* 2015; 2: 54-60.